

Prompt Gamma Activation Analysis (PGAA)

1. Introduction

Forschungsneutronenquelle Heinz Maier-Leibnitz (FRM II) started its operation in 2004. It was built as a replacement of Forschungsreaktor München (FRM), which operated from 1957 to 2000. FRM II is modern multi-purpose research reactor used not just in science, but also in medicine and in the industry.

2. Neutrons

Neutron is subatomic particle, which, together with the proton, forms the atomic nuclei. It has **no electric charge**, its mass is similar to that of the proton ($m_n = 1838.68 m_e$, $m_p = 1836.15 m_e$, where m_e is the mass of the electron). The free neutron is not stable, it decays away with β^- decay ($n^0 \rightarrow p^+ + e^- + \bar{\nu}$, where $\bar{\nu}$ stands for the anti-neutrino) with the half-life of 614 s.

When neutrons are needed, they have to be generated in nuclear reactions like fusion (e.g. ${}^2\text{H} + {}^2\text{H} \rightarrow {}^3\text{He} + n$), or fission. A research reactor uses the **fission** of ${}^{235}\text{U}$ nuclei, during which one thermal neutron is absorbed in the nucleus, and two medium-heavy nuclei are formed, the so-called fission products, together with two or three fast neutrons. The fission-product nuclei are rich in neutrons, they are highly radioactive, and stabilize in subsequent β^- decays with half-lives ranging from a few hundredths of seconds up to millions of years. In 0.7% of fission events, delayed neutrons are also emitted with half-lives of less than a minute. These neutrons are used for the regulation of the chain reaction. The fast neutrons need to be slowed down (**thermalized**) for the maintaining the chain reaction.

The neutrons in the reactor have different energies. The ones produced in the fission are fast, their energies are around 2 MeV. The fuel element is surrounded by heavy water (D_2O), which moderates the fast neutrons. The neutrons in thermal equilibrium with the moderator, are called **thermal neutrons**. Their energy is 0.025 eV on average. The neutrons, which are on the way of thermalization, are called epithermal.

Thermal neutrons in principle follow the Maxwellian distribution, they have the average energy of 0.025 eV, their average wavelength is 1.8 Å, and the average velocity is 2200 m s⁻¹ at the temperature of 293 K (20°C).

In large neutron facilities, the neutrons are further cooled in a secondary moderator. In FRM II, it is about 15 l of liquid deuterium (D_2) with the temperature of about 25 K, which produces the so-called **cold neutrons**.

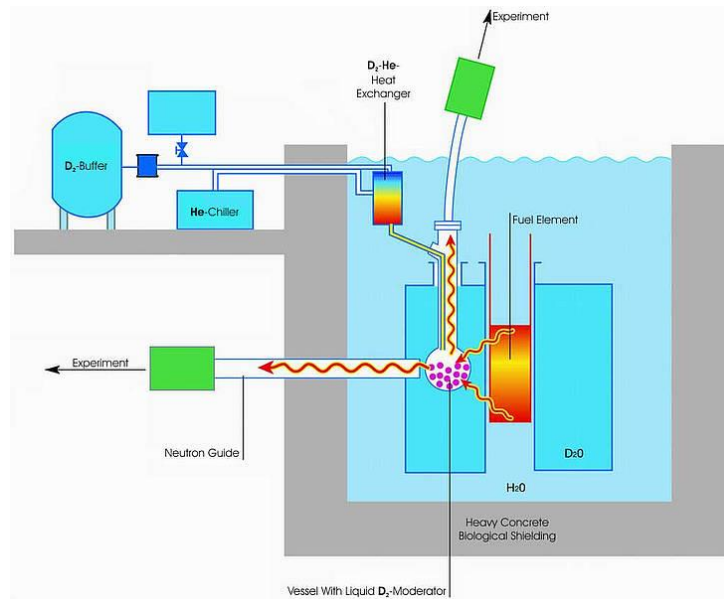


Figure 1. The schematic operation of the cold source in FRM II reactor (source FRM II webpage)

The energies of **cold neutrons** are below 0.005 eV (i.e. much below the typical energies of chemical bonds), their wavelengths are around 5 Å (in the range of crystal lattices), and their velocities are a few hundred m s⁻¹. They are ideal for non-destructive investigations of atomic or nano-structures mainly based on neutron scattering. The neutron flux in the cold source is above 10¹⁴ cm⁻² s⁻¹.

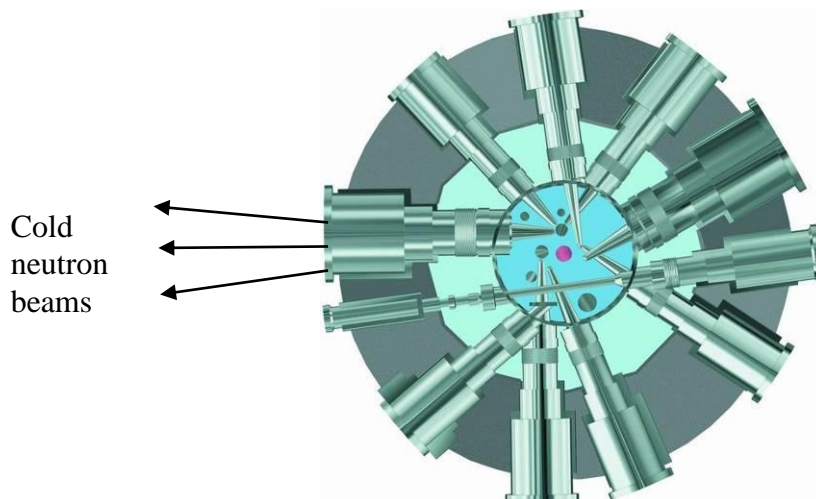


Figure 2. Beam tubes in FRM II reactor (source: FRM II webpage)

Cold neutrons can be transported away from the reactor core using **neutron guides**. When using a simple flight tube, the intensity of the neutron beam decreases according to $1/r^2$. In guides, neutrons can be transmitted with just a very little loss, which is proportional to $1/r$. The inner surface of the guide tubes are covered with the so-called **supermirror** made of hundreds of sub-micron titanium and nickel layers. Each pair of metal layers reflects one wavelength with Bragg reflection, while the whole cover (with the total thickness of a few microns) reflects a whole wavelength range within $\pm 2-3^\circ$. The guides can be as long as 50–100 m. The neutron flux at the end of a guide like this is still more than 10⁹ cm⁻² s⁻¹. The flux

can be further increased with the use of elliptically tapered guides. At the PGAA facility at FRM II the flux at the focal point is $6 \times 10^{10} \text{ cm}^{-2} \text{ s}^{-1}$.



Figure 3. Neutron guides (source: FRM II web page)

3. Radiative neutron capture (or the (n,γ) reaction)

Neutrons have no electric charge, thus they can interact with the positively charged atomic nucleus at any energy. (Not like charge particles, which need energies higher than a given threshold energy.) Whenever a nucleus absorbs a slow (thermal or cold) neutron, a so-called compound nucleus is formed whose excitation energy equals the **binding energy** of the neutron. (In the case of epithermal or fast neutrons, the kinetic energy needs also to be taken into account.) The binding energy is in the range of 6–10 MeV for most nuclei, it tends to increase with the atomic number until $Z = 22\text{--}28$, then slowly decreases. Most compound nuclei get rid of the excitation energy with the emission of γ radiation. This is called radiative neutron capture, or (n,γ) reaction.

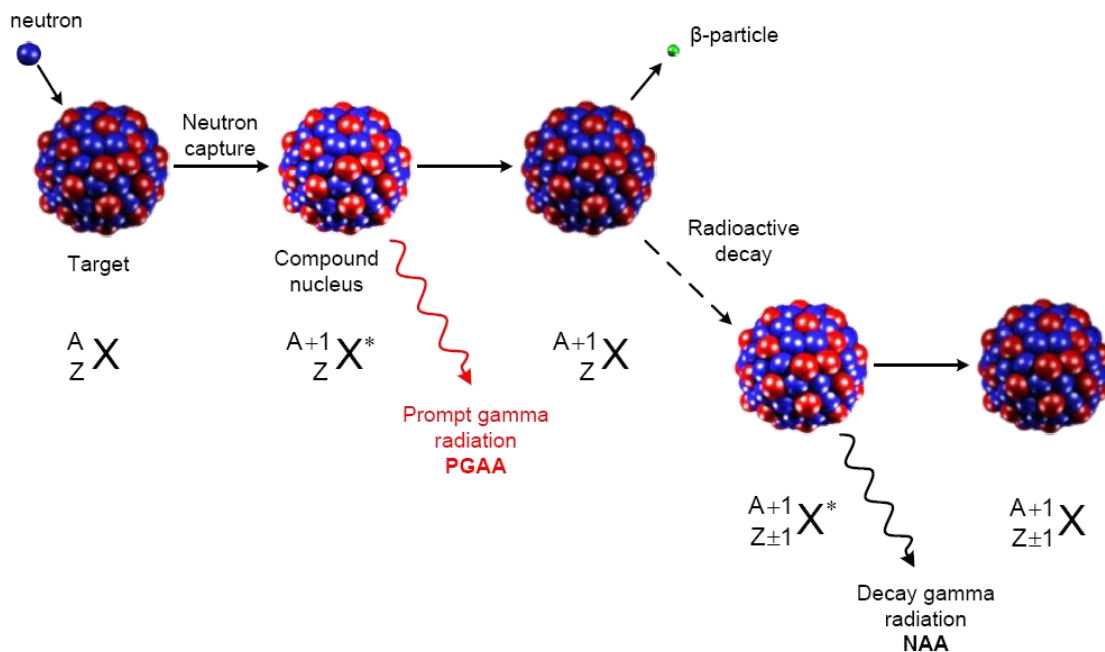


Figure 4. The process of the (n,γ) reaction.

If the nucleus formed in the de-excitation is stable, then the process ends. If it is radioactive, then it decays away typically with β decay with a given half-life, during which **delayed γ radiation** is also emitted. The typical form is β^- decay, as these nuclides are neutron rich, but sometimes β^+ decay can also occur. As a result, we get a nucleus whose mass number increased by one, but the atomic number increased (or in the case of β^+ decay decreased) by one.

After a neutron capture, certain nuclides emit charged particles: the most important reactions are the following: ${}^3\text{He}(n,p){}^3\text{H}$, ${}^6\text{Li}(n,\alpha){}^3\text{H}$, ${}^{10}\text{B}(n,\alpha){}^7\text{Li}$, or ${}^{14}\text{N}(n,p){}^{14}\text{C}$. In the case of neutron capture in ${}^{10}\text{B}$, the first energy level above the ground state of ${}^7\text{Li}$ is also populated, that is why γ radiation with the energy of 478 keV is also emitted. These reactions have rather high probabilities (cross sections), so they are applied in neutron detection or when shielding against neutrons.

The probability of the neutron capture is described by the **neutron capture cross section**. The SI unit of it is cm^2 , but barn = 10^{-24}cm^2 is also accepted. The “real” cross section, as calculated from the sizes of protons and neutrons, is typically between 1–10 barns. While the scattering cross sections of the nuclei are not far from these values, the capture cross section can be several orders of magnitude smaller, or even higher. The nucleus of ${}^4\text{He}$ (i.e. the α particle) is so stable that it does not interact with neutrons at all. This is the only exception in the nature. Other stable nucleus formations typically have very low cross sections, like ${}^{12}\text{C}$ (0.0035 b), ${}^{16}\text{O}$ (0.00019 b), or the ones with closed neutron shells (e.g. ${}^{37}\text{Cl}$, ${}^{40}\text{Ca}$ with $N = 20$, ${}^{90}\text{Zr}$ with $N = 50$, all less than 1 b). On the other hand, there are several nuclides, which “like” to absorb neutrons, i.e. they have high cross sections, such as ${}^{113}\text{Cd}$ (20,600 b), ${}^{157}\text{Gd}$ (257,000 b). These are typically heavy metals far from the magic numbers (meaning the nuclear shells), which have very dense level schemes, and an energy level slightly above the capture state is excited with a high probability (so-called low-energy resonances). Elemental cadmium and gadolinium (together with the above-mentioned boron) are also good neutron shielding materials.

The capture cross section highly depends on the neutrons kinetic energy. The most important rule that describes this correlation is the so-called **$1/v$ law**, which means that the cross section is inversely proportional to the velocity (v), or the square root of the kinetic energy. This law is strictly valid for every nuclide at the cold neutron energies, for most nuclides at thermal neutron energies. The light nuclides follow this rule up until the fast neutron energies. The simple explanation for this phenomenon is that the more time the neutron spends in the vicinity of the nucleus, the higher is the probability of its being absorbed.

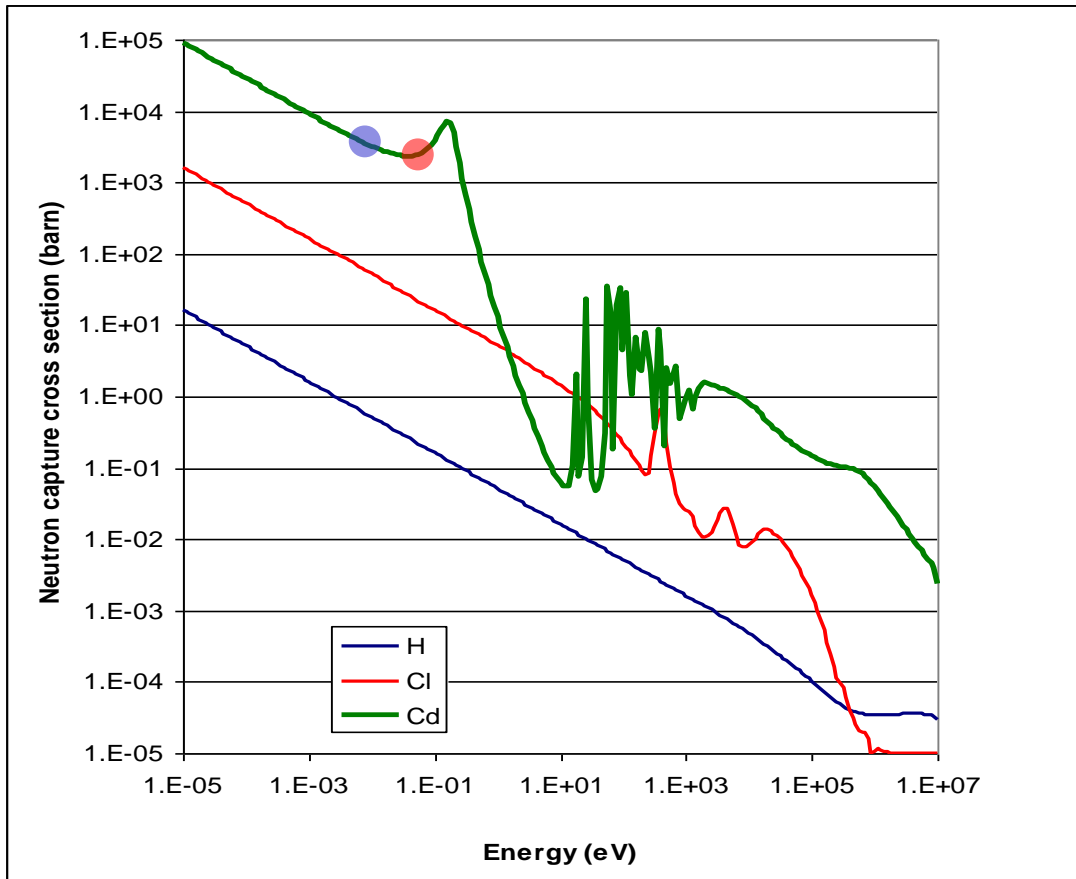


Figure 5. Capture cross sections of H, Cl and Cd as a function of energy.

As can be seen in the above figure, hydrogen (dominant isotope: ^1H) follows the $1/v$ law until about 1 MeV. Chlorine (^{35}Cl) has its first resonance above 100 eV, while in the case of cadmium (^{113}Cd) the first resonance is already at 0.17 eV, which is followed by broad region of unresolved resonances. This low-lying resonance overlaps with the thermal neutron energies. It can also be seen that in the cold-energy range, all cross-section curves are parallel on log-log scale, i.e. their ratios are independent from the neutron energies.

The capture state is not a state in the quantum mechanical point of view, as it lives just for a very short time, decays in about 10^{-14} s, and de-excites in less than 10^{-10} s. This short lifetime is still long enough that all the nucleons share equally the excitation energy (unlike in fast-neutron reactions, where the projectile runs through the nucleus kicking out one or more nucleons), but still far below the resolutions times of the counting devices, and even more below the delayed γ radiation following β decay. The γ radiation emitted during the de-excitation is thus called **prompt gamma radiation**. The total energy released during the de-excitation always equals the binding energy.

There are a few nuclides, where no energy levels exist between the capture state and the ground state. These nuclides always emit their full excitation energy in the form one high-energy prompt gamma photon, like ^1H (2223 keV), ^2H (6250 keV). In all other cases, there is at least one energy level below the capture state; so the de-excitation goes through an energy cascade.

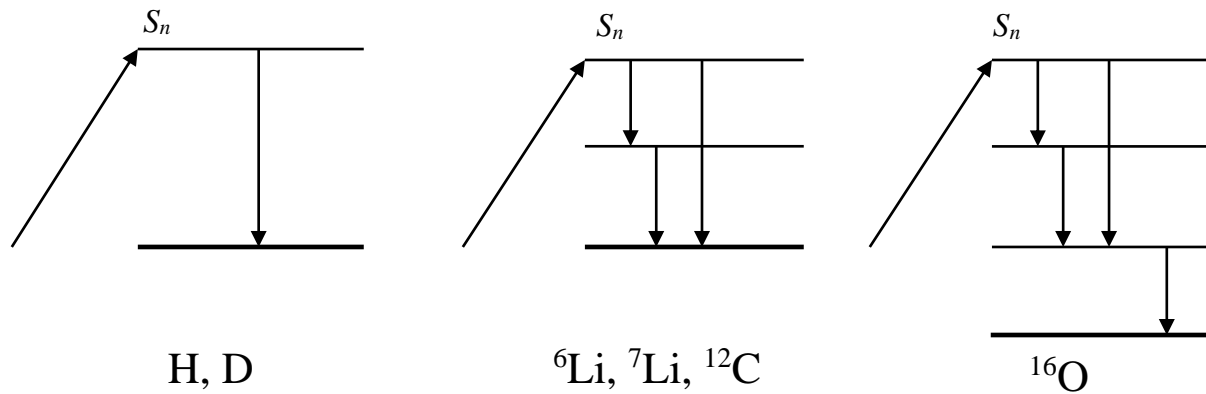


Figure 6. De-excitation from the capture state for a few light nuclides (S_n stands for the neutron binding energy).

The energies of the gamma photons correspond to the differences between the level energies, thus they are characteristic to the emitter nuclide. (The gamma energy is slightly smaller than the energy of the transition due to the recoil of the nucleus, but the deviation is typically less than 1 keV.) The **branching ratios**, i.e. the probabilities of the transitions from a certain level depend on the nuclear properties of the states (spins, parities etc.).

The gamma rays appear in the spectra as peaks at certain energies. Heavier elements can have hundreds or thousands of levels below the capture state, at certain energy ranges sometimes they can be regarded as a continuum. The gamma spectra of these elements have **characteristic peaks** (close to the binding energy showing the primary transitions, and at low energies, showing the transitions to the ground state), but broad regions of irresolvable peaks also appear in them (see below).

The **emission probability** of a given γ photon is mainly determined by the branching ratio of the transition. At low energies, however, electrons might be emitted instead of gamma rays (electron conversion, EC)

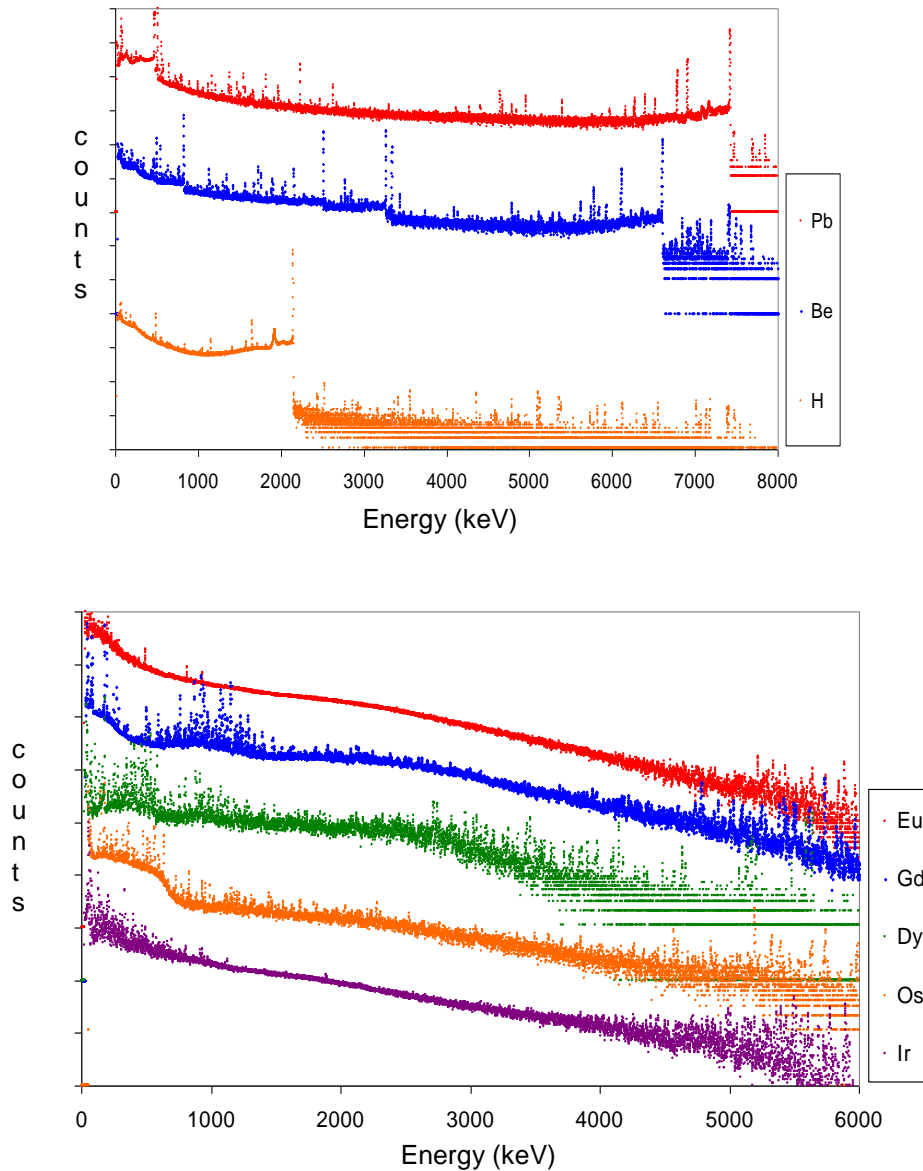


Figure 7. Spectra with strong characteristic peaks, with lower-intensity background peaks (above) and with many irresolvable peaks and broad continuum (below).

4. Chemical analysis based on radiative neutron capture

All the chemical elements emit a series of characteristic prompt gamma rays, based on which they can be identified in the gamma spectra. Because of the large number of peaks, interferences may disturb the identification. That is why several of the strongest peaks need to be found to detect one element with a high certainty. Not just the energies, but also the **relative intensities** are characteristic. If we find a handful of peaks, whose energies agree with those of the element, and they also show the same intensity pattern, then we can regard the element as detected.

Once an element has been identified, the amount of it in the irradiated sample can be determined as follows:

$$\frac{A}{\varepsilon t} = aP_\gamma = n \Phi_0 \theta \sigma_0 P_\gamma = \frac{m}{M} N_A \Phi_0 \sigma_\gamma \quad (1)$$

where A is the peak area, ε is the counting efficiency, t is the measurement time (live time, s). The ratio $A/\varepsilon t$ shows the number of gamma photons emitted by the element in the irradiated sample in a second; it is sometimes called γ activity.

- 1) It equals the activity (a , number of decays per second) times the emission probability (P_γ).
- 2) When the activity is generated in a nuclear reaction, n is the number of atoms from the given element, which equals the mass m (g) over the molar mass M (g/mol) times the Avogadro constant N_A (mol^{-1}). Φ ($\text{cm}^{-2} \text{s}^{-1}$) is the flux of the neutron beam. At the end of the expression, the nuclear constants appear: θ is the isotopic abundance, σ is the neutron capture cross section, while P_γ is the emission probability of the given gamma ray (mostly agrees with the branching ratio, discussed above).
- 3) The product of this three cannot be determined independently in this method, hence we use one unified constant σ_γ , which is called the **partial gamma-ray production cross section**. The '0' index shows that the flux and the cross sections are regarded at thermal energies. The unit of the cross sections is cm^2 in this equation.

The activation equation in (1) is the basic equation for the **absolute method** of prompt gamma activation analysis (PGAA). Any quantity can be determined, if all the others are known. First, we have to calibrate our detection system with calibration sources of known activities and emission probabilities. Once we know the efficiency, with a flux monitor, whose mass and partial cross section are known, we can determine the flux. Then, if we know the partial cross section of an element for a given gamma peak, we can determine its mass. Alternatively, if we know the mass, then we can determine partial cross section for later analyses.

As the cross section is energy dependent, it seems important to differentiate between irradiations in cold and thermal beams. As mentioned above, the cross section ratios are constant over the energy range of slow neutrons. This phenomenon can be used to simplify the flux determination. If we use the thermal cross section of a flux monitor to determine the flux, we use a number about 4-times too low, and thus we get an increased flux value. That is called the **thermal-equivalent flux**. If we use thermal-equivalent fluxes and thermal cross sections, our calculations will always be consistent independent of the actual energy distribution of the neutron beam. (There is one exception, when a neutron beam's energy range overlaps with a range in the cross section, where the $1/v$ law is not valid anymore due to a low-resonance resonance. In this rare case, a special correction factor is taken into consideration to account for the discrepancy. In the frame of this lab practice, we do not deal with such cases.)

Sometimes we cannot be sure of the beam flux reaching the sample actually. The beam might be inhomogeneous, too, and we cannot measure the average flux exactly at the same location and shape as for the sample. We might not know the actual mass, either, because the sample itself can be larger than the beam. In such cases, we can still use the **relative method** of PGAA, i.e. we can use a simplified version of equation (1) as follows:

$$\frac{A_1 / \varepsilon_1}{A_2 / \varepsilon_2} = \frac{n_1 \sigma_{\gamma,1}}{n_2 \sigma_{\gamma,2}} \quad (2)$$

where on the right-hand side we can see the efficiency corrected peak area ratio which equals the molar ratio times the partial cross section ratio. The measurement time and the flux cancel. The molar ratio can easily be calculated to mass ratio, too: $m_1/m_2 = n_1/n_2 \times M_1/M_2$. The relative method can be regarded as using an internal flux monitor chosen from the components of the sample, but the flux is not explicitly expressed.

From the mass ratios or the molar ratios, the composition can be calculated either in weight percent or in molar percent. With the relative method, we do not get the actual mass of the element in the irradiated sample. It makes other simplifications possible, too. As we do not need the absolute efficiency, just the efficiency ratio, we do not need to use absolute activities during the calibration, which are sometimes known just with a relatively high uncertainty.

If we calculate the concentration from equation 1, and disregard the uncertainties from flux, time, and efficiency, then we also follow the relative method in the end.

The relative method makes very simple to determine partial cross sections, too: one just needs to irradiate a simple compound, whose **stoichiometric coefficients** are very well known. Then from the efficiency-corrected peak-area ratio, one can simply determine the unknown cross section relative to the other.

We can also use the delayed γ radiation for analysis as well, as the **delayed gammas** are also characteristic. The energy released after activation is typically less than 3 MeV, which results in much less transition, and thus much simpler spectra. When the counting takes place after the irradiation, one has to correct for the decay using these three factors:

$$S = 1 - e^{-\lambda t_{act}} \quad (3)$$

$$D = e^{-\lambda t_{cool}} \quad (4)$$

$$C = \frac{1 - e^{-\lambda t_{count}}}{\lambda t_{count}} \quad (5)$$

where $\lambda = \ln 2 / T_{1/2}$ (the half-life in seconds), t_{act} , t_{cool} , and t_{count} mean the activation, cooling, and counting times, respectively. The **saturation activity** can be calculated from the dividing the activity on the left-hand side in equations 1 by the product of these three factors.

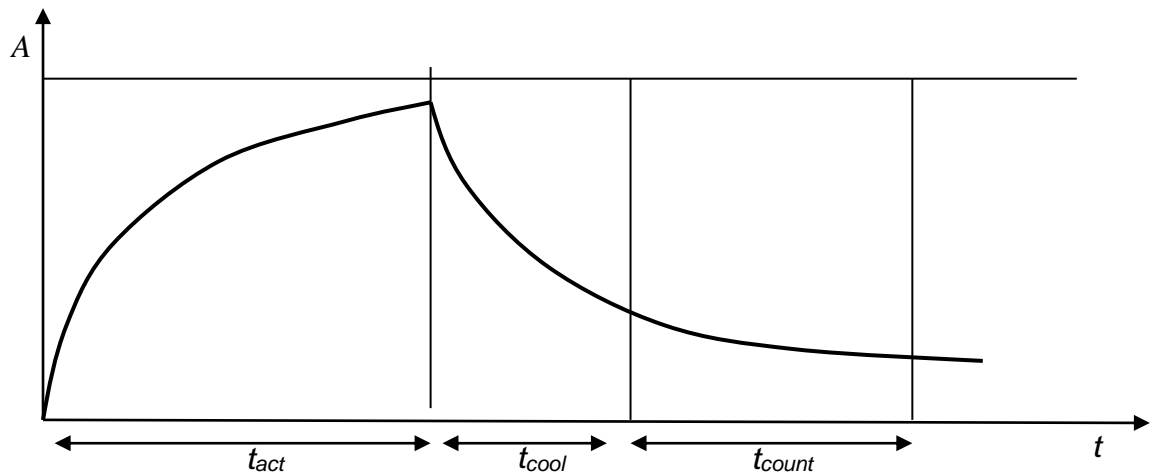


Figure 8. The change of activity in time during and after the activation. The thin horizontal line represents the saturation activity.

This method is called the **neutron activation analysis (NAA)**. The irradiations take place in a near-core irradiation channel, while the counting is performed in low-background laboratories, where the samples are transferred with pneumatic transfer systems. The strong cold beam at FRM II can be used for activation very efficiently.

If the counting is performed simultaneously with the irradiation, then we use the in-beam correction factor alone:

$$B = 1 - \frac{1 - e^{-\lambda_{count} t}}{\lambda_{count} t} \quad (6)$$

5. Gamma spectroscopy

Gamma radiation is acquired by a gamma spectrometer. The soul of this system is the **high-purity germanium (HPGe) semiconductor detector**.

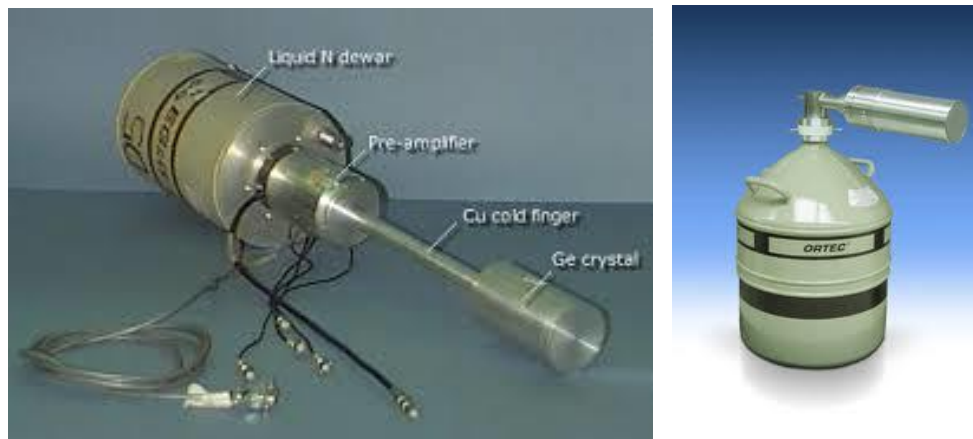


Figure 9. HPGe detectors

It can be regarded as a large (100–200 cm³) diode, which is biased in the terminating direction, i.e. no electric current is flowing in it. Once ionizing radiation produces electron-hole pair in its volume, a weak current can be observed. To minimize the disturbing effects from the thermal noise, the detector is kept at the temperature of liquid nitrogen. The detector signal is amplified and its height, that is proportional to the absorbed energy, is determined by a **digital spectrometer**. After the evaluation of one signal, the spectrometer adds one count to a channel proportional to this signal height (in the end to the gamma energy) in the so-called **multi-channel analyzer (MCA)**. The spectra we use contain 16384 channels, we collect photons between about 30 keV and 11 MeV, thus one channel is about 0.7 keV broad. The total number of counts is typically many millions. The spectrometer handles **count rates** up to a few ten thousands counts per second (cps), but is typically operated at a few thousand cps.

The detector does not directly detect the γ photons. In the interaction of the photon with matter (see below), energetic charged particles (electrons, and sometimes also positrons) are produced. They generate a large number of electron-hole pairs in the semiconductor crystal. Counting is a statistical procedure, which results in a more-or-less Gaussian peak, whose Full Width at the Half of Maximum (FWHM) is 0.1–0.3% of the energy (at 1332 keV, large

detectors, like the one at FRM II, have an FWHM of 1.9 keV, but using the low gain typical for PGAA it is somewhat worse: 2.3 keV).

The spectrum of a mono-energetic γ ray does not contain only one single line in the spectrum. The detector response function depends on the interactions of the photons with the germanium crystal, which are the following:

1. **Photo-electric effect.** In this interaction, the total energy of the γ photon is transmitted to an atomic electron, whose energy will be fully absorbed, and a signal proportional to this absorbed energy will be seen at the output. Photo-electric effect is typical for low-energy (max. few hundred keV) photons. If a photon is immediately absorbed in the crystal in one photo-electric effect, we will see a count appearing at the energy of the photon (E).
2. **Compton scattering.** In Compton scattering, only a fraction of the photon energy will be transmitted to an atomic electron, and a lower-energy scattered photon will also be released. This photon may leave the crystal, or can interact with it again. Compton scattering is the typical interaction of medium-energy photons (max. a few MeV). If the photon undergoes only Compton scattering, then the respective count will appear somewhere below the photon energy. That is why we see a broad Compton plateau in each spectrum. Compton scattering is not isotropic. Its highest probability is for forward scattering, when there is no energy loss, and the backward scattering, when the energy loss is the greatest, and the back scattered photon has the energy of about 250 keV (a bit less than the half of the electron's rest mass). When this photon leaves the detector, a count will appear ~ 250 keV below E .
3. **Pair production.** This is typical for high-energy photons, i.e. with the energy of several MeV. In this case, an electron-positron pair is produced in the vicinity of an atom. Both charged particles loose their kinetic energies fully. After slowing down, the positron annihilates on an atomic electron producing (in most cases) two γ photons with the energy of exactly 511 keV (which is the rest mass of the electron), flying in the opposite directions. Any of the two photons may or may not interact and thus be detected in the detector. If one of them does not, but the other is fully absorbed, then a peak will appear at the energy of $E - 511$, if none of them do, then a second peak appears also at $E - 1022$. They are called single and double escape peaks, respectively.

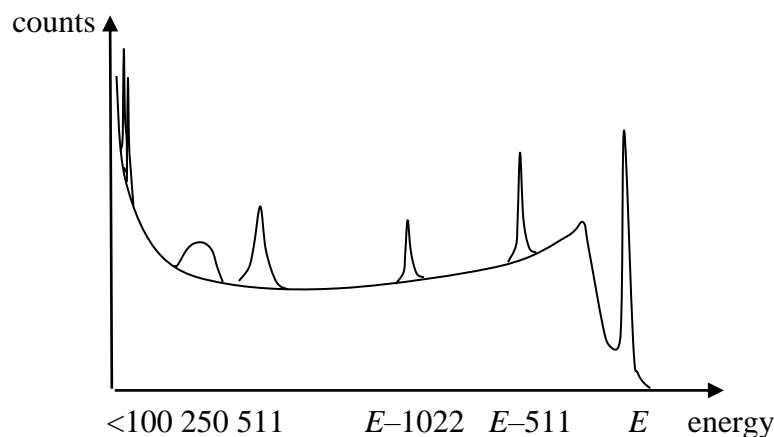


Figure 10. Schematic drawing of the detector response function.

The effects of all three interactions can be observed in the **detector response function** (see the figure above). The full-energy peak at E means the events, during which the whole photon energy is absorbed in the detector in one or several steps. The two escape peaks can be seen at the energies of $E-511$ and at $E-1022$. The so-called annihilation peak can be seen at 511 keV, which originate from escape photons from the structural materials. The energy of the Compton electrons are between 0 and $E - 250$, that is why the Compton plateau starts at very low energies and ends half way between the single escape peak and the full-energy peak in the form of the so-called Compton edge. Between this and the full-energy peak, events from multiple Compton scatterings appear. The photons back-scattered from the structural materials, produce a broad peak around 250 keV. Below 100 keV, one can see x-ray peaks induced by the gamma radiation in the structural materials and in the detector.

The Compton plateau can be significantly reduced by a solution called **Compton suppression**. A scintillator detector (in our case bismuth germanate, BGO, see figure below) surrounds the HPGe detector in order to catch the scattered photons.

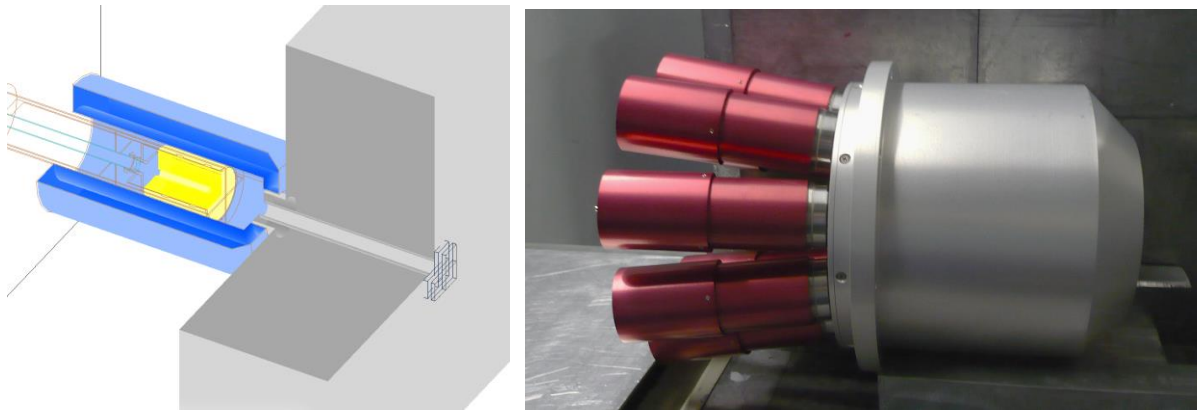


Figure 11. Bismuth germanate (BGO) scintillator surrounding the HPGe detector used for Compton suppression, design and photo.

Scintillators are another typical detector type in nuclear measurements. They emit a light flash in visible-ultraviolet range while being ionized. The light is collected by mirrors to a converter, which emits electrons, and so-called photo-multiplier tubes amplify this weak current for further handling by electronics. The most well-known scintillators are zinc sulfide (ZnS), sodium iodide (NaI), and bismuth germanate (BGO).

The detector system is surrounded by a thick lead shielding (see figure below), which also serves the purpose that the BGO does not see any other radiation, just the one scattered out from the HPGe.



Figure 12. Shielding of the sample chamber.

Whenever the two detectors fire at the same time, a Compton event has just happened, meaning energy loss. If those events are rejected, the spectrum will be much cleaner. Compton suppression can efficiently reduce the Compton plateau, thus smaller characteristic peaks can be detected all over the spectrum, as can be seen in the next figure.

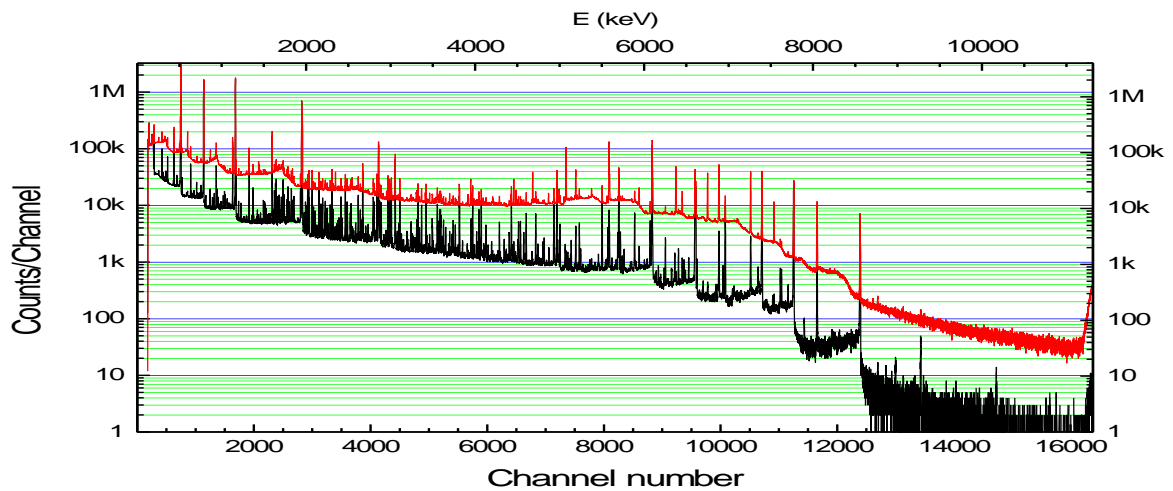


Figure 13. Normal and Compton-suppressed prompt gamma spectra of Cl (PVC).

Once the Compton suppression is operational, we can start collecting spectra. The spectrum can be regarded as a vector, whose elements are integers. In our context, these numbers are counts in channels. To assign physical meaning to this set of counts, one has to calibrate the spectrum. The calibration remains valid until the system is changed, but it needs to be checked from time to time. (The PGAA instrument is calibrated at the beginning of each cycle.)

The spectrum peaks can then be fit using several programs, which determine the net peak areas, see below.

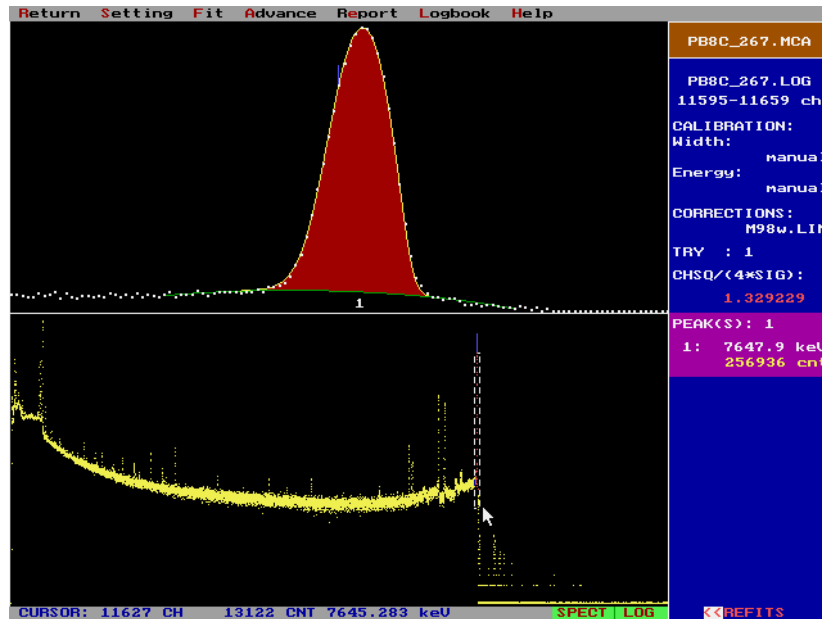


Figure 14. Peak fitting with Hypermet-PC.

To assign the channels to photon energy is called the **energy calibration**, when calibration sources are measured, whose photon energies are accurately known. Then we need to determine the detector efficiency, which shows the fraction of γ photons collected at a given energy compared to actual number of photons emitted by the sample. The detector at the PGAA facility is located at the distance of 330 mm from the sample, which means that we detect only a very small fraction (less than 0.1%) of the photons. At about 100 keV, the photons are detected for sure, once they reach the detector, but high-energy photons are detected with a much smaller probability. The detector efficiency involves both the geometric and the intrinsic efficiency. The **efficiency** curve for the PGAA detector at FRM II can be seen in the next figure.

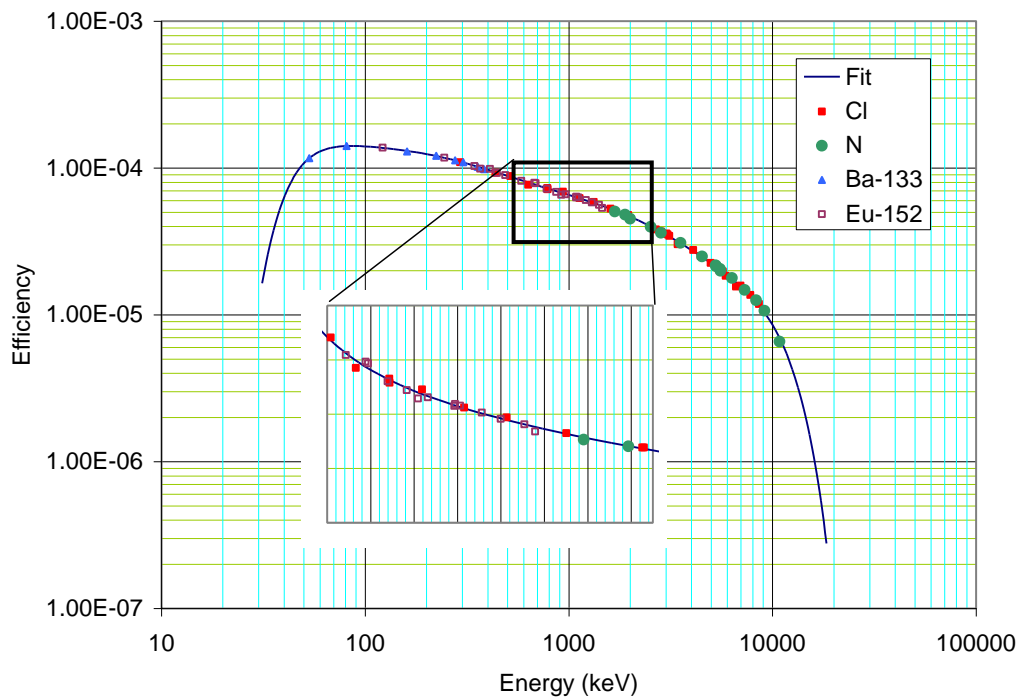


Figure 15. **Efficiency** of the HPGe detector.

The **chemical analysis** is normally performed using a dedicated program. During the analysis, one has to identify all the chemical elements whose strongest lines appear in the spectrum (**qualitative analysis**). Then the masses have to be calculated according to equation 1 (**quantitative analysis**). In case of several strong lines, an average mass can be determined. The equivalent masses of the background components (lead from the shielding, fluorine from the Teflon sample holder, aluminum from sample chamber, etc.) have to be subtracted from the masses. These masses can be obtained from the chemical analysis of background spectra. From the net masses, one can then determine the composition of the sample using the relative method of chemical analysis.

6. PGAA instrument at FRM II

Neutron guides and collimators. The neutron beam arrives from the cold source through an approx. 55-m long, curved neutron guide, whose last 7 m is elliptically tapered. (The curvature filters out fast neutrons and gamma radiation arriving from the core.) The last 110-cm long section can be replaced with a collimator. In the first case one gets a strong focused beam (thermal-equivalent flux up to $6 \times 10^{10} \text{ cm}^{-2} \text{ s}^{-1}$), while in the second case, a weaker homogeneous beam is the result (flux up to $3 \times 10^9 \text{ cm}^{-2} \text{ s}^{-1}$). The beam size is maximum $20 \times 20 \text{ mm}^2$.

The **sample chamber** is made of aluminum and is lined from inside with ^6Li -containing plastic (to absorb the scattered neutrons). It can be evacuated. It is equipped with sample changer: a carousel with 16 positions, from where aluminum sample frames can be moved into the beam. The samples are attached to the frames with Teflon string, and are typically sealed in Teflon (CF_2) bags.

The anti-Compton detector system (HPGe surrounded by BGO) is placed perpendicularly to the beam. The sample-to-detector distance is 330 mm. The radiation emitted by the sample reaches the HPGe detector through a lead collimator with an aperture diameter of 20 mm.

Behind the sample chamber, a **beam stop** is located. It is made of boron carbide. It absorbs the thermal neutrons while emitting 478-keV γ photons, which are shielded against with lead. (1 cm of lead attenuates the 478-keV gamma rays from neutron capture on boron with about an order of magnitude.)

The whole instrument is covered with about 3 t of **lead** to **shield** against the strong radiation from the neutron guide, the beam stop, and the sample. The layout can be seen below.

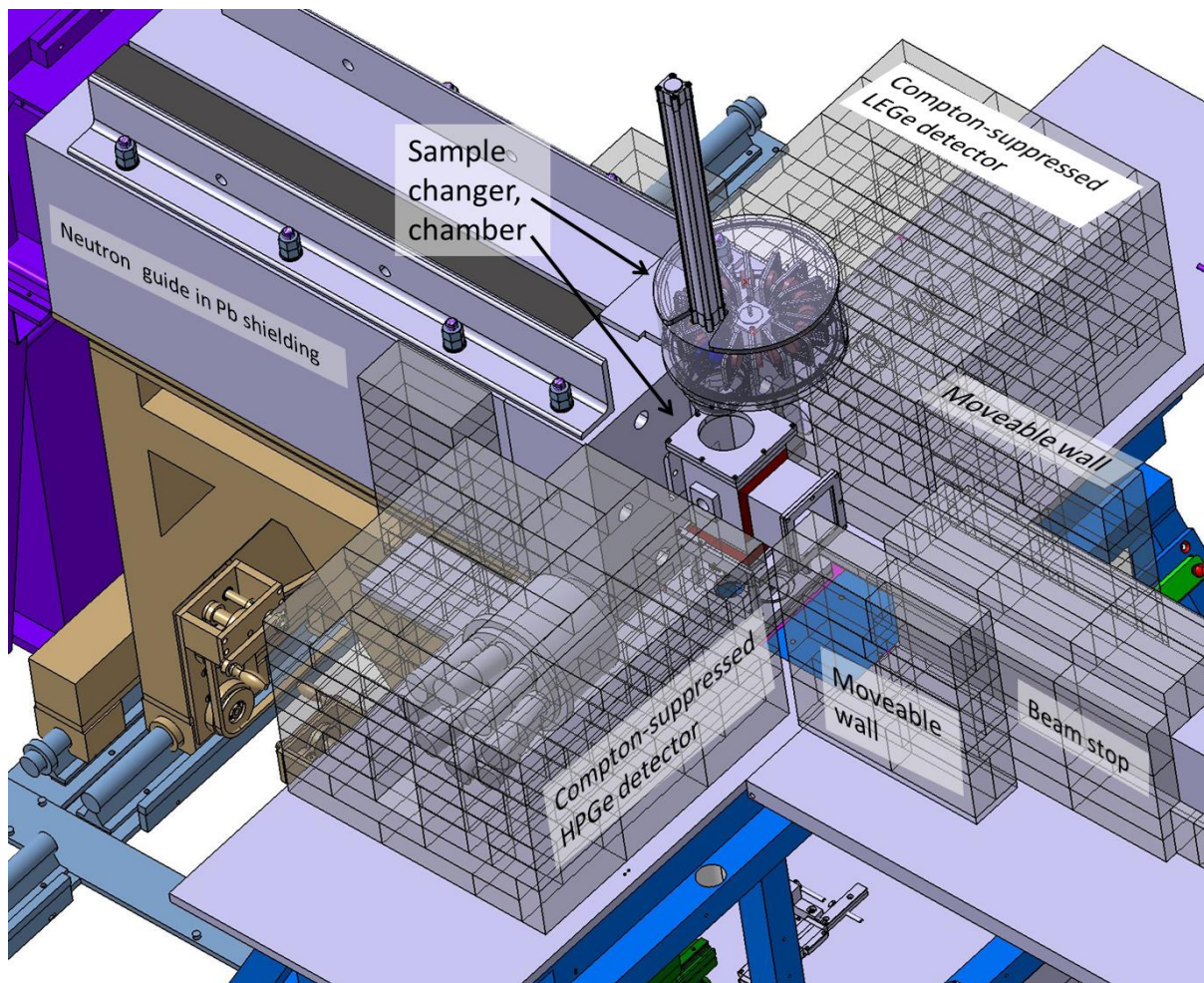


Figure 16. The layout of the PGAA facility. (Lead shielding and neutron guide removed around the neutron beam.)

7. Tasks

1. Determine the efficiency of the detector at selected energies using a ^{152}Eu source.

Activity of the source: $393.0 \text{ kBq} \pm 1.5\%$ at 2008-03-01 (1st of March, 2008), its half-life: 13.516 y.

Plot the data points in log-log scale, then fit a straight line to it, and use this function in the later tasks.

Table 1. Energies and emission probabilities together with their uncertainties for ^{152}Eu (also available in excel file).

Energy (keV)	Emission probability (%)
121.7817 (3)	28.41 (13)
244.6974 (8)	7.55 (4)
344.2785 (12)	26.58 (12)
411.1165 (12)	2.237 (10)
778.9045 (24)	12.96 (6)
867.380 (3)	4.241 (23)
964.079 (18)	14.49 (6)
1085.837 (10)	10.13 (6)
1089.737 (5)	1.73 (1)
1112.076 (3)	13.40 (6)
1212.948 (11)	1.415 (9)
1299.142 (8)	1.632 (9)
1408.013 (3)	20.84 (9)
1457.643 (11)	0.498 (4)

2. Determine the thermal-equivalent neutron flux at the sample position with a titanium flux-monitor foil using the efficiencies from task 1. (Take care of the units!)

mass: 0.00275g

molar mass: 47.87 g/mol

cross section at 342 keV: $1.84 \text{ barn} \pm 1.1\%$

cross section at 1381 keV: $5.18 \text{ barn} \pm 2.3\%$

(efficiency at 342 keV in Feb 2019: $0.000161 \pm 1.6\%$)

(efficiency at 1381 keV in Feb 2019: $8.13 \times 10^{-5} \pm 1.8\%$)

3. Determine the partial gamma-ray production cross section for 770-keV line of potassium from the PGAA spectrum of potassium chloride (KCl) using the relative method. Prepare and measure the sample, evaluate the lines at 770 keV and at 517 keV. Calculate the partial cross section and estimate the uncertainty of the result.

cross section: Cl 517 keV σ_γ : $7.58 \pm 0.6\%$

(efficiency ratio in Feb 2019): $\varepsilon(770)/\varepsilon(517) = 1.211 \pm 0.7\%$

4. Prepare a sample of cement, measure it with PGAA. Collect prompt (and decay) spectra. In the spectrum viewer, identify the major components of the sample (using the databases available at the instrument), i.e. make the qualitative analysis. Determine the composition based on the strongest lines of the identified elements, i.e. perform the quantitative analysis on the sample.

Table 2. Molar masses of elements for $Z < 30$, efficiencies at different energies (from Aug 2014, efficiency ratios are approximately valid at any time), partial gamma-ray production cross sections for the prompt (and certain decay) gamma lines. (Also available in Excel.)

Z	EI	MW	E(keV)	dE	$\epsilon(b)$	$d\epsilon\%$	σ	$d\sigma\%$	RI	T1/2 (s)
1	H	1.008	2223.259	0.019	5.76E-05	1.2	3.33E-01	0.2	100.0	
3	Li	6.941	2032.31	0.07	6.1E-05	1.1	3.98E-02	5	100.0	
3	Li	6.941	980.559	0.046	8.65E-05	0.4	4.36E-03	5.1	11.0	
3	Li	6.941	1051.817	0.048	8.43E-05	0.4	4.36E-03	5.1	11.0	
4	Be	9.012	853.631	0.011	9.1E-05	0.5	1.65E-03	8.9	26.7	
4	Be	9.012	3367.484	0.035	4.22E-05	1.5	2.92E-03	8.9	47.3	
4	Be	9.012	2590.014	0.025	5.17E-05	1.3	1.88E-03	8.9	30.4	
4	Be	9.012	6809.579	0.099	2.17E-05	1.4	6.18E-03	9	100.0	
5	B	10.811	477.6	5	0.000112	0.6	7.13E+02	0.3	100.0	
6	C	12.011	1261.708	0.057	7.82E-05	0.5	1.23E-03	2.7	45.6	
6	C	12.011	4945.302	0.066	3.01E-05	1.4	2.70E-03	2.9	100.0	
6	C	12.011	3684.016	0.069	3.91E-05	1.5	1.17E-03	3.5	43.5	
7	N	14.007	1884.853	0.031	6.38E-05	1.0	1.45E-02	1.3	61.1	
7	N	14.007	5268.984	0.072	2.83E-05	1.4	2.37E-02	1.5	100.0	
7	N	14.007	5297.662	0.153	2.81E-05	1.4	1.67E-02	1.6	70.5	
7	N	14.007	5533.251	0.076	2.7E-05	1.3	1.57E-02	1.6	66.0	
7	N	14.007	6322.301	0.088	2.35E-05	1.3	1.49E-02	1.7	62.8	
7	N	14.007	10829.102	0.208	1.04E-05	4.8	1.07E-02	3.5	44.9	
8	O	15.999	870.682	0.034	9.04E-05	0.5	1.75E-04	6.2	99.8	
8	O	15.999	1087.714	0.031	8.32E-05	0.4	1.51E-04	6.3	85.9	
8	O	15.999	2184.381	0.039	5.82E-05	1.2	1.50E-04	6.2	100.0	
8	O	15.999	3272.109	0.069	4.32E-05	1.4	3.53E-05	7.1	20.1	
9	F	18.998	1633.602	0.015	6.91E-05	0.8	9.60E-03	4.3	100.0	11.2
9	F	18.998	583.493	0.022	0.000104	0.6	3.52E-03	4.3	36.7	
9	F	18.998	655.942	0.022	9.98E-05	0.6	1.96E-03	4.3	20.5	
9	F	18.998	6600.386	0.11	2.25E-05	1.3	9.85E-04	5.2	10.3	
11	Na	22.99	1368.633	0.006	7.55E-05	0.6	5.30E-01	1.6	18.5	53852
11	Na	22.99	90.979	0.016	0.000176	1.7	2.65E-01	1.3	45.1	
11	Na	22.99	869.221	0.017	9.04E-05	0.5	1.13E-01	1.2	20.8	
11	Na	22.99	6395.048	0.126	2.33E-05	1.3	1.01E-01	2	19.3	
12	Mg	24.305	584.936	0.024	0.000104	0.6	3.16E-02	4.7	100.0	
12	Mg	24.305	1808.616	0.059	6.54E-05	1.0	1.81E-02	4.7	57.3	
12	Mg	24.305	2828.117	0.105	4.85E-05	1.4	2.39E-02	4.7	75.6	
12	Mg	24.305	3916.653	0.157	3.71E-05	1.5	3.14E-02	4.7	99.5	
12	Mg	24.305	3053.85	0.117	4.56E-05	1.4	8.27E-03	4.8	26.2	
13	Al	26.982	1778.85	0.03	6.6E-05	1.0	2.33E-01	1.3	99.4	134.5
13	Al	26.982	7723.782	0.255	1.86E-05	1.5	6.67E-02	2	28.7	
14	Si	28.086	3538.976	0.05	4.05E-05	1.5	1.18E-01	1.7	100.0	
14	Si	28.086	4933.826	0.074	3.01E-05	1.4	1.12E-01	2	95.3	
14	Si	28.086	1273.383	0.029	7.79E-05	0.6	2.89E-02	1.9	24.5	
14	Si	28.086	2092.914	0.032	5.99E-05	1.1	3.30E-02	1.9	28.0	
14	Si	28.086	6379.747	0.107	2.33E-05	1.3	2.10E-02	2.8	17.8	
14	Si	28.086	7199.016	0.127	2.04E-05	1.4	1.27E-02	3.1	10.8	
15	P	30.974	77.992	0.023	0.000171	1.6	5.89E-02	4.8	74.4	
15	P	30.974	512.65	0.018	0.000109	0.6	7.92E-02	5	100.0	
15	P	30.974	636.57	0.017	0.000101	0.6	3.10E-02	4.6	39.1	
15	P	30.974	1071.154	0.02	8.37E-05	0.4	2.48E-02	4.7	31.3	
15	P	30.974	3899.648	0.076	3.72E-05	1.5	3.01E-02	4.7	38.0	
16	S	32.066	841.013	0.014	9.15E-05	0.5	3.48E-01	1.7	100.0	
16	S	32.066	2379.495	0.035	5.5E-05	1.3	2.08E-01	1.5	59.9	
16	S	32.066	5420.241	0.1	2.75E-05	1.4	3.09E-01	2.3	88.9	
16	S	32.066	3220.364	0.057	4.37E-05	1.4	1.24E-01	1.6	35.8	
17	Cl	35.453	517.077	0.008	0.000109	0.6	7.43E+00	0.9	83.2	
17	Cl	35.453	1164.831	0.012	8.09E-05	0.5	8.92E+00	0.7	100.0	
17	Cl	35.453	788.37	0.212	9.36E-05	0.5	4.90E+00	2	55.0	
17	Cl	35.453	786.182	0.15	9.37E-05	0.5	3.61E+00	2	40.5	
17	Cl	35.453	1951.15	0.015	6.25E-05	1.1	6.49E+00	0.8	72.7	
17	Cl	35.453	1959.359	0.016	6.24E-05	1.1	4.18E+00	0.9	46.9	
17	Cl	35.453	6110.711	0.072	2.44E-05	1.3	7.37E+00	1.4	82.6	
17	Cl	35.453	6619.576	0.081	2.24E-05	1.3	2.75E+00	1.6	30.8	
17	Cl	35.453	7790.277	0.106	1.84E-05	1.5	2.89E+00	2.1	32.4	
17	Cl	35.453	6627.865	0.084	2.24E-05	1.3	1.56E+00	1.9	17.5	
17	Cl	35.453	8578.583	0.153	1.61E-05	1.8	9.28E-01	2.8	10.4	
19	K	39.098	770.325	0.023	9.44E-05	0.5	9.03E-01	1.3	100.0	
19	K	39.098	1158.88	0.024	8.11E-05	0.5	1.60E-01	1.6	17.7	
19	K	39.098	1618.976	0.029	6.95E-05	0.8	1.30E-01	1.6	14.4	

Z	El	MW	E(keV)	dE	$\epsilon(b)$	$d\epsilon\%$	σ	$d\sigma\%$	RI	T1/2 (s)
20	Ca	40.078	1942.677	0.027	6.27E-05	1.1	3.52E-01	2.1	100.0	
20	Ca	40.078	519.563	0.075	0.000108	0.6	5.03E-02	2.6	14.3	
20	Ca	40.078	2001.314	0.029	6.16E-05	1.1	6.59E-02	2.3	18.7	
20	Ca	40.078	6419.694	0.213	2.32E-05	1.3	1.76E-01	2.6	50.0	
20	Ca	40.078	4418.497	0.12	3.33E-05	1.4	7.08E-02	2.6	20.1	
21	Sc	44.956	147.114	0.016	0.00017	1.6	6.08E+00	1.4	85.2	
21	Sc	44.956	227.86	0.016	0.000149	1.0	7.13E+00	1.5	100.0	
21	Sc	44.956	142.627	0.016	0.000171	1.6	4.88E+00	1.5	68.5	
21	Sc	44.956	295.343	0.019	0.000135	0.7	3.97E+00	2.8	55.6	
22	Ti	47.88	1381.738	0.027	7.51E-05	0.6	5.18E+00	2.3	100.0	
22	Ti	47.88	341.689	0.029	0.000127	0.6	1.84E+00	1.1	35.6	
22	Ti	47.88	1585.952	0.027	7.02E-05	0.8	6.24E-01	1.2	12.1	
22	Ti	47.88	6760.011	0.089	2.19E-05	1.4	2.97E+00	2.9	57.3	
22	Ti	47.88	6418.353	0.08	2.32E-05	1.3	1.96E+00	2.9	37.8	
23	V	50.942	1434.06	0.01	7.38E-05	0.7	4.95E+00	2.1	99.0	224.58
23	V	50.942	125.234	0.027	0.000175	1.7	1.61E+00	2.6	32.5	
23	V	50.942	645.789	0.022	0.0001	0.6	7.69E-01	2.2	15.6	
23	V	50.942	6517.617	0.148	2.28E-05	1.3	7.83E-01	5.5	15.8	
23	V	50.942	7163.168	0.181	2.05E-05	1.4	5.90E-01	7.3	11.9	
24	Cr	51.996	834.803	0.033	9.17E-05	0.5	1.38E+00	1.9	100.0	
24	Cr	51.996	749.102	0.032	9.53E-05	0.5	5.69E-01	1.5	41.3	
24	Cr	51.996	7937.858	0.117	1.8E-05	1.6	4.24E-01	2.5	30.8	
24	Cr	51.996	8510.681	0.137	1.63E-05	1.8	2.31E-01	3.5	16.7	
24	Cr	51.996	8482.84	0.14	1.64E-05	1.8	1.68E-01	4.2	12.2	
25	Mn	54.938	846.754	0.02	9.13E-05	0.5	1.28E+01	1.2	62.9	9280
25	Mn	54.938	83.884	0.023	0.000174	1.6	3.11E+00	1.6	24.2	
25	Mn	54.938	1810.72	0.04	6.53E-05	1.0	3.63E+00	2.7	17.8	9280
25	Mn	54.938	7243.518	0.092	2.02E-05	1.4	1.36E+00	2.4	10.6	
26	Fe	55.847	352.332	0.016	0.000126	0.6	2.73E-01	1.2	41.8	
26	Fe	55.847	122.078	0.022	0.000175	1.8	9.56E-02	3.1	14.7	
26	Fe	55.847	691.914	0.016	9.79E-05	0.6	1.37E-01	1.3	20.9	
26	Fe	55.847	7631.051	0.093	1.89E-05	1.5	6.53E-01	1.9	100.0	
26	Fe	55.847	7645.485	0.093	1.89E-05	1.5	5.49E-01	2	84.0	
26	Fe	55.847	9297.903	0.207	1.42E-05	2.3	7.47E-02	3.3	11.4	
27	Co	58.933	229.811	0.012	0.000148	1.0	7.18E+00	1.2	100.0	
27	Co	58.933	277.199	0.011	0.000138	0.8	6.77E+00	1.2	94.2	
27	Co	58.933	555.941	0.01	0.000106	0.6	5.76E+00	1.1	80.3	
27	Co	58.933	447.717	0.011	0.000115	0.6	3.41E+00	1.1	47.6	
27	Co	58.933	7491.29	0.121	1.94E-05	1.5	1.16E+00	2.5	16.1	
28	Ni	58.69	464.972	0.018	0.000113	0.6	8.43E-01	1.2	56.6	
28	Ni	58.69	8998.31	0.093	1.5E-05	2.1	1.49E+00	1.9	100.0	
28	Ni	58.69	8533.453	0.083	1.62E-05	1.8	7.21E-01	1.9	48.4	
28	Ni	58.69	6837.437	0.064	2.16E-05	1.4	4.58E-01	1.7	30.8	
28	Ni	58.69	7819.547	0.075	1.84E-05	1.5	3.37E-01	1.9	22.7	
29	Cu	63.546	277.993	0.025	0.000138	0.8	8.93E-01	1.3	100.0	
29	Cu	63.546	159.018	0.026	0.000167	1.5	6.49E-01	1.2	72.7	
29	Cu	63.546	185.658	0.026	0.00016	1.3	2.44E-01	1.3	27.3	
29	Cu	63.546	202.689	0.026	0.000155	1.2	1.94E-01	1.3	21.7	
29	Cu	63.546	343.651	0.025	0.000127	0.6	2.15E-01	1.5	24.1	
29	Cu	63.546	7915	0.088	1.81E-05	1.5	8.69E-01	1.9	97.3	
30	Zn	65.39	115.256	0.023	0.000176	1.8	1.67E-01	1.6	47.0	
30	Zn	65.39	1077.336	0.017	8.35E-05	0.4	3.56E-01	1.4	100.0	
30	Zn	65.39	7863.545	0.107	1.82E-05	1.5	1.41E-01	3.5	39.7	